ISSN: 1698-6180
www.ucm.es/info/estratig/journal.htm

Journal of Iberian Geology 32 (2) 2006: 215-231

Journal of Iberian Geology
AN INTERNATIONAL PUBLICATION OF EARTH SCIENCES

Coupled microbial and geochemical reactive transport models in porous media: Formulation and Application to Synthetic and *In Situ* Experiments

Modelos acoplados de transporte reactivo con procesos geoquímicos y microbiológicos en medios porosos: Formulación y aplicación a experimentos *in situ* y sintéticos

J. Samper[1]*, G. Zhang[2], L. Montenegro[1]

[1]E.T.S. Ingenieros de Caminos, Canales y Puertos, Universidad de A Coruña, Campus de Elviña s/n, 15192 A Coruña, Spain
[2]Earth Sciences Division, Lawrence Berkeley National Laboratory, 1 Ciclotron Road, CA-94720, USA

**Corresponding author: jsamper@udc.es*

Received: 22/05/06 / Accepted: 12/07/06

Abstract

The study of natural groundwater chemistry and contamination as well as the safety assessment of underground disposal facilities for radioactive waste require the use of models which are able to consider simultaneously groundwater flow, heat transfer, solute transport, geochemical reactions and microbiological processes. This paper presents a mathematical and numerical formulation of coupled water flow and microbial reactive transport in porous media which has been implemented in a coupled biogeochemical reactive transport code, BIO-CORE$^{2D©}$ by adding microbiological processes into a nonisothermal reactive transport code, CORE$^{2D©}$. BIO-CORE$^{2D©}$ incorporates efficient numerical algorithms such as a first-order unconditionally-stable implicit version of the sequential iteration approach and a sophisticated automatic time stepping algorithm which optimizes the size of the time step. Hydrobiogeochemical models are illustrated with a synthetic example and the CERBERUS experiment performed at the Mol underground research laboratory in Belgium to evaluate the effect of heat and radiation on Boom clay.

Keywords: Reactive transport, microbial processes, numerical model, BIOCORE

Resumen

El estudio de la calidad natural y la contaminación de las aguas subterráneas así como la evaluación de la seguridad de las instalaciones subterráneas de almacenamiento de residuos radiactivos requiere utilizar modelos acoplados de flujo subterráneo, transporte de calor y solutos, reacciones químicas y procesos biológicos. Este artículo presenta la formulación matemática y numérica del modelo acoplado de flujo y transporte reactivo con procesos biológicos para medios porosos que ha sido implementada en el código BIO-CORE$^{2D©}$ mediante la adición de los procesos microbiológicos en el código de transporte reactivo no isotermo CORE$^{2D©}$. BIO-CORE$^{2D©}$ incorpora algoritmos numéricos eficientes para resolver la versión cuasi implícita del método de iteración secuencial y determinar de forma automática los intervalos de tiempo óptimos. Se presentan modelos hidrobiogeoquímicos para una columna sintética y para el experimento *in situ* CERBERUS realizado en el laboratorio subterráneo de Mol en Bélgica para evaluar el efecto del calor y la radiación en la arcilla de Boom.

Palabras clave: Transporte reactivo, procesos microbianos, modelo numérico, BIOCORE

1. Introduction

Quantitative analyses of groundwater chemistry and contamination require the use of models which can handle simultaneously groundwater flow, heat transfer, solute transport, geochemical reactions and microbiological processes. Sophisticated numerical models have been developped in recent years for multicomponent reactive solute transport, but they rarely consider thermal and microbiological processes. On the other hand, existing microbiological models of porous media do not account for thermal and geochemical effects in a comprehensive manner.

1.1. Coupled microbiological and geochemical reactive transport codes

Brun (1997) summarized 28 reactive transport codes which account for microbial processes. Essaid and Bekins (1997) developed BIOMOC, a code that solves for groundwater flow and solute transport in 2-D porous media coupled with multiple degradation processes and microbial populations, including sequential biodegradation formulated either by single, multiple, or minimum Monod kinetics (Monod, 1949). Salvage and Yeh (1998) presented BIOKEMOD, a code which copes with an unlimited number of substrates, electron acceptors and microbes. They coupled abiotic geochemical processes to subsurface microbial processes. Initially, this code considered only batch processes, but later was extended to deal with transport processes, resulting in HBGC123D (Salvage and Yeh, 1999). HBGC123D deals with coupled non-isothermal hydrologic transport and kinetic and/or equilibrium biogeochemical reactions in variably saturated media. It solves iteratively for 1-, 2-, or 3-D water flow, solute and heat transfer equations, and the ordinary differential and algebraic equations of mixed biogeochemical reactions. Hunter *et al.* (1998) presented BIORXNTRN, a code which considers a comprehensive set of microbially-driven geochemical processes and describes microbially-driven geochemical zonation. Chilakapati *et al.* (2000) presented RAFT, a code for 3-D water flow and reactive transport coupled with biological processes. Advanced automatic code generation and automatic built-in parameter estimation are also some outstanding features of this code.

Battistelli (2004) coupled an existing numerical reservoir simulator, TMVOC (Pruess and Battistelli, 2002) and BIOMOC (Essaid and Bekins 1997), leading to TMVOCbio, to simulate the biodegradation of organic contaminates under multiphase conditions.

Some codes can handle changes in subsurface properties induced by microbial activity such as bioclogging. Engesgaard (2000) presented a code (BIOCLOG3D) dealing with biodegradation and biological processes in 3-D media. A code (MISER) simulating the coupled physical, chemical and bioclogging processes in soil vapor extraction and bioventing system has been developed by Rathfelder *et al.* (1999) which can be used to perform quantitative analyses of remediation of unsaturated soils.

1.2. Approaches for coupling solute transport and chemical reactions

Approaches for solving reactive transport problems are quite diverse. In general, three major approaches have been used (Yeh and Tripathi, 1989) which include: (1) Coupling existing geochemical or microbiological code to solute transport codes; (2) Direct Substitution (DSA) of the nonlinear chemical reactions into the transport equations leading to a set of nonlinear Partial Differential Equations (PDE's); and (3) Operator Splitting and Sequential Iteration Approach (SIA) in which linear transport PDE's and nonlinear Algebraical Equations (AE's) are solved sequentially in an iterative manner (multiple-step method or SIA) or without iterations (two-step method or operator splitting).

No method has proven to be better than others. The general philosophy of multicomponent reactive transport modeling is discussed in depth by Rubin and James (1973), Rubin (1983), Kirkner and Reeves (1988), and Reeves and Kirkner (1988) among others. These authors describe various solution methods and identify optimal approaches suitable for specific chemical reactions. The numerical efficiency of these three approaches has been compared by Xu (1996), Lichtner *et al.* (1996) and Saaltink *et al.* (2001). In addition, some variations of SIA were developed. For example, an improved sequential iteration approach (SIA-1; Tebes-Stevens *et al.* 1998; Zhang, 2001) was proven to be more efficient for modeling microbial processes and kinetically-controlled geochemical processes; A Sequential Non-Iteration Approach (SNIA) was used to model slow flow, transport and geochemical processes with high efficiency and acceptable accuracy (Xu *et al.*, 2006).

In the direct substitution approach, chemical equations are incorporated directly into the transport equations. This approach has been employed by, among others, Valocchi *et al.* (1981); Jennings *et al.* (1982); Miller and Benson (1983); Carnahan (1990); Steefel and Lasaga (1990); Xu (1996); Saaltink *et al.* (1997).

The two-step operator splitting method divides the solution into a transport step where aqueous components are

transported individually by advection and dispersion and a chemical step where aqueous and solid components react with each other. The two steps are coupled either sequentially or iteratively. Since the sets of equations that are solved simultaneously are much smaller than those of the direct approach, larger systems with larger sets of chemical components can be handled with the two-step method.

According to Xu (1996) SIA has advantages with respect to the direct substitution approach for chemically complex large-size reactive transport problem. On the other hand, the DSA can yield high accuracy for a limited number of chemical species and reactions. Its disadvantage is the very high demand on computing resources, which limits the number of components, species, and reactions that can be handled (Yeh and Tripathi, 1989; Mangold and Tsang, 1991). Saaltink *et al.* (2001) also presented a comparison of the two methods. He concluded that DSA performs better numerical efficiency than SIA for chemically complex small dimensional reactive transport problems while DSA is worse for chemically-simple large-dimensional problems. However, as pointed out by Cederberg *et al.* (1985), the sequential iteration approach (SIA) takes advantage of the fact that only the physical transport equations are spatially connected, while chemical equations depend strictly on local conditions at each point in the system.

In order to improve the global convergence behavior of the sequential iteration approach, Tebes-Stevens *et al.* (1998) proposed a modified sequential iteration approach which is based on a first-order approximation of the chemical rate by a Taylor expansion of the rate in terms of concentrations of primary species. This linearization of the highly non-liner chemical rates allows one to substitute the chemical equations directly into the transport equations. If derivative terms with respect to concentrations of other components, apart from the component for which the rate is calculated, are ignored, the size of the transport matrix is the same to that of a standard SIA. However, the global convergence behavior is greatly improved. Tebes-Stevens *et al.* (1998) implemented this improved sequential iteration approach, which is denoted SIA-1, into FEREACT to deal with Monod kinetics for biodegradation processes and found that SIA-1 performs much better than the standard method. SIA-1 has been adopted in BIO-CORE$^{2D©}$ to deal with chemical kinetics and it has been found also to perform much better than standard SIA.

1.3. Methods for Coupling Microbial Kinetics

Early approaches to deal with microbial processes treated microorganisms as immobile phases colonizing on the surface of the solid matrix. The diffusion limitation of aqueous substrates to microbial colonies was not considered. On the other hand, bioengineers and hydrologists have paid much attention to attached microorganisms, but ignored geochemical processes. Their models focused on substrate availability in biofilms. Some models employ a diffusion equation to simulate substrate availability in biofilms (Molz *et al.*, 1986). Some codes use empirical and simple algebraic equations instead of the general diffusion PDE (Brun, 1997). The simplest method adopted in BIOGLOD3D (Engesgaard, 2000) assumes that the substrate concentration in biofilm is proportional to the bulk concentration and the proportionality factor needs to be calibrated.

Aqueous phase microbes, which tend to equilibrate with attached biomass, have been considered in some codes such as BIOKEMOD (Salvage and Yeh, 1998) and BIOCLOD3D (Engesgaard, 2000). Aqueous phase microbes are subject to transport processes and induce chemical processes. Most existing codes consider neither the diffusive limitation of substrates in biofilms nor the interactions among microorganisms such as growth competition, cometabiosis and endogenous respiration,

However, groundwater, especially shallow or organic-rich groundwater, harbours enough microorganisms, and biofilm is ubiquitous (Lewandowski, *et al.*, 1994), and the microbial flora in subsurface ecosystem is diverse. Therefore, both the diffusive resistance of biofilms and interactions among microorganisms are relevant. Only a few codes consider interactions among microorganisms (Salvage and Yet, 1998). The diffusive resistance of biofilm is considered in some models in an oversimplified manner (Molz, 1986; Engesgaard, 2000). In order to overcome these limitations Zhang (2001) developed BIO-CORE$^{2D©}$ a code designed to deal with biogeochemical reactive transport for a diversity of subsurface microbial flora and accounting for biofilms and interactions among microbes. In addition to flow, transport, and geochemical and microbiological processes, BIO-CORE$^{2D©}$ incorporates a single layer diffusive biofilm model to account for the diffusive resistance, introduced by the attached biomass (immobile), for substrates, electron acceptors and other nutrients species from the solution, while dissolved biomass is considered to be in direct contact with available dis-

solved substrates, electron acceptors and nutrients. Details of the biofilm model incorporated in BIO-CORE$^{2D©}$ can be found in Zhang (2001).

BIO-CORE$^{2D©}$ (Zhang, 2001; Zhang and Samper, 2001b) was developed by adding a numerical module for structured and distributed, multiple microbial component ecosystem, into a geochemical reactive transport code, CORE$^{2D©}$ (Samper *et al.*, 2003a). BIOCORE^{2D} has been verified against other codes and has been used to interpret the Redox Zone experiment in a fracture zone of the Äspö site (Samper *et al.*, 2003a; Molinero *et al.*, 2004) and evaluate the role of microbial processes in oxygen depletion after closure of a HLW repository in crystalline rocks (Samper *et al.*, 2006a). BIOCORE^{2D} has been improved recently by Samper *et al.* (2003b) and Yang (2006).

1.4. Scope

The mathematical formulation of water flow, solute transport and geochemical processes is presented first. Then, a description of subsurface microbial ecosystems, microbial kinetics, mobility and metabolic rates is presented. Numerical methods used for solving this formulation are presented next. Main features and capabilities of BIO-CORE$^{2D©}$ are described. Applications of hydrobiogeochemical models to a synthetic example and the CERBERUS *in situ* experiment are then described.

2. Mathematical formulation of flow and multicomponent reactive transport

The governing equation for flow in variably saturated porous media is given by (Bear, 1979):

$$\nabla \cdot \left[K_r K \nabla(\psi + z)\right] + w = (\phi \frac{\partial S_w}{\partial \psi} + S_w S_s) \frac{\partial \psi}{\partial t} \quad (1)$$

where t is time, ψ is pressure head, w is a fluid source/sink per unit volume of medium, K_r is relative conductivity, K is saturated hydraulic conductivity, S_w is water saturation defined as the ratio of volumetric water content θ to porosity ϕ (for fully saturated media $S_w = 1$), S_s is storativity, and $\nabla\cdot[\ ]$ and $\nabla(\ )$ are divergence and gradient operators, respectively. Our formulation assumes that under unsaturated conditions there is only flow of liquid water, although gas pressures are allowed to vary in space in a manner prescribed by the user (Xu *et al.*, 1999; Samper *et al.*, 2003a). For aqueous systems, 'multi-species reactive transport' can be reduced to 'multi-component reactive transport' (Yeh and Tripathi, 1991; Walter *et al.*, 1994; Steefel and Lasaga, 1994) if diffusion and dispersion coefficients are the same for all aqueous species. Transport equations for chemical components can be expressed as (Xu *et al.*, 1999):

$$\nabla \cdot (\theta \mathbf{D} \nabla C_i) - \mathbf{q} \cdot \nabla C_i + w(C_i^* - C_i) + \theta R_i = \theta \frac{\partial C_i}{\partial t}$$
$$i = 1, 2, ..., N_c \quad (2)$$

where C_i is total dissolved concentration of the i-th chemical component, $\boldsymbol{D}$ is the dispersion tensor, C_i^* is the dissolved concentration of water source w, N_c is the number of chemical components and R_i is the reactive sink/source term which includes all the chemical interactions of the i-th component with solid or gas species. These primary governing equations need to be complemented with constitutive chemical relationships, which are local equations relating secondary variables to primary variables.

Dissolved species are subject to transport in liquid phase as well as to chemical interactions with other aqueous species (homogenous reactions), and solid species (heterogeneous reactions).

Not all chemical species are strictly needed to fully describe a chemical system. Usually, a subset of N_c chemical species is selected as components or primary species. Secondary species can be written as linear combinations of primary species (Parkhurst *et al.*, 1980; Yeh and Tripathi, 1991).

By assuming local equilibrium for aqueous complexation, acid-base and redox reactions, the mass action law allows one expressing the concentration of secondary species x_j in terms of those of primary species, c_i, according to (Xu *et al.*, 1999; Samper *et al.*, 2003a):

$$x_j = K_j^{-1} \gamma_j^{-1} \prod_{i=1}^{N_c} c_i^{\nu_{ji}} \gamma_i^{\nu_{ji}} \quad (3)$$

where K_j is the equilibrium constant, x_j and c_i are concentrations and γ_j and γ_i are thermodynamic activity coefficients.

Sorption of solutes at solid surfaces can be described by means of cation exchange and surface complexation models. Details of such models can be found elsewhere (Dzombak and Morel, 1990; Appelo and Postma, 1993; Samper *et al.*, 2003a). Under local equilibrium conditions, dissolution-precipitation reactions can be described by the law of mass action. Dissolution-precipitation reactions which are slow compared to relevant transport and other geochemical processes must be modeled using kinetic rate expressions (Lasaga *et al.*, 1994; Ayora *et al.*, 1995).

3. Formulation of microbial processes

3.1. Definition of microbial system

Microbial growth depends strongly on substance and energy supply from the environment. Microbes gain mass by assimilating carbon compounds and energy by oxidizing carbon or other compounds. Inorganic carbon species such as bicarbonate, methane and carbon dioxide are products of microbial metabolism. Dissolved oxygen, nitrate, Mn (IV), Fe(III), sulfate and carbon dioxide are used as electron acceptors. Microbial processes usually control the redox potential of the system. Microbial growth depends also on environmental factors such as temperature, pressure, pH and Eh (Rheinheimer *et al.*, 1992). Endogeneous respiration is a process by which cell reserves are used as substrates when other organic substrates are not available.

To mathematically describe the subsurface ecosystem, let N_b be the total number of microbial species, N_s the number of substrates, N_a the number of electron acceptors and N_n the number of nutrients in the system. A set of indicator variables are introduced to define the links among microbial and chemical species of a given microbial ecosystem. A given microbial species *i* may grow on one or more substrates. Let N_b^i be the number of growth processes for the *i*th microbe with $1<N_b^i<N_n$. Each growth process involves a substrate, an electron acceptor and a nutrient. It should be noticed that a microbe can grow using a given substrate and relying on several electron acceptors. Similarly, $I_s(i,j)$ is the substrate used by the *i*th microbe in its *j*th growth process and $I_a(i,j)$ denotes the electron acceptor used by the *i*th microbe in its *j*th growth process to feed from the $I_s(i,j)$-substrate. By the same token, $I_n(i,j)$ denotes the nutrient involved in the *j*th growth process of the *i*th microbe. Using matrix notation, these indicators $I_s(i,j)$, $I_a(i,j)$ and $I_n(i,j)$ can be arranged in three matrices $\mathbf{I_s}$, $\mathbf{I_a}$ and $\mathbf{I_n}$.

To illustrate the use of this notation let us consider a system containing 2 microbial species, B_1 and B_2, 3 substrates, S_1, S_2 and S_3, 2 electron acceptors, A_1 and A_2 and 3 nutrients, N_1, N_2 and N_3. B_1 has 3 growth processes, $N_b^1=3$, by using substrates S_1, S_1 and S_2 correspondingly using A_1, A_2 and A_1 as electron acceptors and N_1, N_2 and N_3 as nutrients, respectively. B_2 has 2 growth processes, $N_b^2=2$, by using S_2 and S_3 as substrates, A_1 and A_2 as electron acceptors and N_2 and N_2 as nutrients, respectively. Then, matrices $\mathbf{I_s}$, $\mathbf{I_a}$ and $\mathbf{I_n}$. are given by

$$\mathbf{I}_s=\begin{bmatrix}1 & 1 & 2\\ 2 & 3 & 0\end{bmatrix}\quad \mathbf{I}_a=\begin{bmatrix}1 & 2 & 1\\ 1 & 2 & 0\end{bmatrix}\quad \mathbf{I}_n=\begin{bmatrix}1 & 2 & 3\\ 2 & 2 & 0\end{bmatrix}$$

3.2. Microbial kinetics

Main biological processes taking place in subsurface microbial ecosystems include: 1) Biomass growth, 2) Oxidation and consumption of substrates, 3) Reduction of electron acceptors and 4) Transformation of nutrients.

Biomass growth is the dominant mass transformation process. Grown biomass comes mostly from consumed substrates. Microbial mass produced in microbial metabolic processes from consumed substrates may be small compared to organic consumption (around 0.01%) or rather large (up to 90%). In some cases biomass growth can be partly contributed by nutrients and electron acceptors. Most dead cells volatilize causing bio-venting. Some of them precipitate on aquifer matrix causing bio-clogging and a few of them are temporarily suspended in groundwater and may finally flow out of the aquifer.

Microbial growth rate depends on four main factors: 1) Its inherent generative power usually measured by the specific generation time or specific growth rate; 2) Its concentration defined as microbial population per unit volume of water; 3) Concentrations of substrates, electron acceptors and nutrient species; and 4) Environmental factors such as temperature, pH and Eh.

If environmental conditions are favorable to microbes, their growth depends only on their inherent generative capacity. In practice, however, microbial growth depends also on the availability of substrates, electron acceptors and nutrients. Monod kinetics takes into account these limitations.

If microbes are only present in the aqueous phase, the overall microbial rate is equal to the sum of the rates of microbial growth, metabolic decay and endogenous respiration:

$$\frac{\partial C_b^i}{\partial t}=\frac{\partial C_b^i}{\partial t}\Big|_{growth}+\frac{\partial C_b^i}{\partial t}\Big|_{decay}+\frac{\partial C_b^i}{\partial t}\Big|_{endogenous} \qquad (4)$$

where C_b^i is the aqueous concentration of the ith microbe in the system. Subscript b refers to biotic species. Microbial growth rate can be written as:

$$\frac{\partial C_b^i}{\partial t}\Big|_{growth}=\sum_{k=1}^{N_b^i} G^{i,k}M^{i,k}C_b^i \qquad (5)$$

where $G^{i,k}$ is the microbial growth factor of *i*th microbe in its *k*th growth phase, which is equal to the product of: (1) the growth constant $K_b^{i,k}$ (T^{-1}), (2) the lag factor $G_L^{i,k}$ which accounts for the time elapsed since a microbe encounters a substrate to the time it is able to build the en-

zymatic systems required to use it and, (3) environmental limitations $G_T^{i,k}$ (temperature) and $G_{pH}^{i,k}$ (pH). Metabolic lag is the time elapsed since a microbe encounters a substrate to the time it is able to build the enzymatic systems required to use it. This process is empirically described by the following function (Salvage and Yeh, 1998):

$$G_L = \begin{cases} 0 & \text{if } T_k \le T_l \\ \dfrac{T_k - T_l}{T_e - T_l} & \text{if } T_l < T_k < T_e \\ 1 & \text{if } T_K \ge T_e \end{cases} \quad (6)$$

where G_L is the lag factor of microbe growth rate (dimensionless), T_k is the time the microbe is exposed to the substrate, T_l is the time needed to start growing after exposure to the substrate and T_e is the time needed to reach exponential growth. $M^{i,k}$ is the overall limiting factor of the *k*th growth process and is equal to the product of the limitation factors of substrates (subindex *s*), electron acceptors (subindex *a*), and nutrients (subindex *n*):

$$M^{i,k} = M_s^{i,k} M_a^{i,k} M_n^{i,k} \quad (7)$$

where $M_s^{i,k}$ is the dimensionless limitation factor of the substrate involved in the *k*th growth process for the *i*th microbe. Let p be the substrate number involved in such growth process. Then, $M_s^{i,k}$ is given by

$$M_s^{i,k} = \frac{C_s^p}{K_s^p S_s^p + C_s^p + C_c^p} \quad (8)$$

where C_s^p is the concentration of the *p*th substrate, K_s^p is the half-saturation constant and S_s^p is a substrate inhibition/stimulation factor which is greater than 1 for inhibition and less than 1 for stimulation. This factor takes into account the effect of chemical or physical factors on the availability of substrates. C_c^p is a competition and/or metabiosis factor for the *i*th microbe which accounts for interactions among two or more microbial species when they: 1) cooperate or depend on each other to use the same substrate (metabiosis); or 2) compete for the same 'food' and space (competition). The competition/metabiosis factor is described by:

$$C_c^p = \sum_{j=1,\neq i}^{N_b} K_c^{i,p,j} C_b^j \quad (9)$$

where $K_c^{i,p,j}$ is the metabiosis (negative value) or competition (positive value) coefficient of the *j*th microbe with respect to the *i*th microbe in its *k*th growth process. This coefficient takes non-zero values only when microbes j and i use the same substrate.

In a similar manner, $M_a^{i,k}$ is the dimensionless limitation factor for the *q*th electron acceptor which is given by:

$$M_a^{i,k} = \frac{C_a^q}{K_a^q + C_a^q} \quad (10)$$

where C_a^q and K_a^q are concentration and half-saturation constant of the *q*th electron acceptor, respectively. Finally, $M_n^{i,k}$ is the dimensionless limitation factor for *r*th nutrient which is given by

$$M_n^{i,k} = \frac{C_n^r}{K_n^r + C_n^r} \quad (11)$$

where C_n^r and K_n^r and are concentration and half-saturation constant of the *r*th nutrient, respectively.

Metabolic decay or biological death obeys first-order kinetics:

$$\frac{\partial C_b^i}{\partial t}\Big|_{decay} = -K_d^i C_b^i \quad (12)$$

where K_d^i is the decay rate of the *i*th microbe.

Endogenous respiration is the process by which microbes consume cell reserves in the absence of sufficient substrates and continue to use the *ie*th electron acceptor. Its rate is given by:

$$\frac{\partial C_b^i}{\partial t}\Big|_{endogenous} = -k_e^i C_b^i \frac{C_a^{ie}}{K_a^{ie} + C_a^{ie}} \quad (13)$$

where C_a^{ie} is the concentration of the *ie*th electron acceptor that can be used by microbe i. Endogenous respiration occurs only when the substrate is short in the system, but the system contains enough electron acceptors. This process, however, can maintain microbes alive at a background biomass concentration.

Microbial metabolism depends strongly on environmental variables such as temperature, pressure, turbidity, pH, Eh, and concentrations of organic and inorganic compounds. The dependence on concentrations of organic and inorganic matters is taken into account by growth limitation factors. The effect of Eh is in fact taken into account in the limitations of electron acceptors. The effects of turbidity and pressure are much less pronounced and can be disregarded. The effects of temperature and pH are most relevant and can be accounted for using formulations such as those described by Zhang (2001).

The overall rate of change of the concentration of the *i*th microbe is given by:

$$\frac{\partial C_b^i}{\partial t} = \sum_{k=1}^{N_b^i} G_k^{i,k} M^{i,k} C_b^i - K_d^i C_b^i - k_e^i C_b^i \frac{C_a^{ie}}{K_a^{ie} + C_a^{ie}} \quad (14)$$

3.3. Coupling microbial and geochemical kinetics

Since microbial processes involve consumption of substrates, reduction of electron acceptors and transformation of nutrients, microbial processes are coupled with geochemical or abiotic processes through yield coefficients. The yield coefficient is defined as the ratio of microbial growth rate to that of substrate consumption. If microbes rely on several substrates then each substrate holds its own yield coefficient according to its contribution to the overall growth. Consumed substrates not used for biomass growth constitute the products of microbial metabolism, which can be CO_2, organic acids, or CH_4. Yield coefficients range from 10^{-4} to 0.9 depending on the type of microorganisms, substrates and other environmental factors. Changes in concentrations of substrates can be calculated from microbial growth rates by means of yield coefficients. The rate of consumption of the *p*th substrate due to microbial processes, B_p, is given by:

$$B_p = \frac{\partial C_s^p}{\partial t} = -\sum_{i=1}^{N_b}\sum_{j=1}^{N_b^i} \frac{1}{Y_s^{i,j,p}} \frac{\partial C_b^i}{\partial t}\Big|_{growth} \quad (15)$$

where $Y_s^{i,j,p}$ is the yield coefficient of the *p*th substrate being used by the *i*th microbe in its *j*th growth process.

The amount of electron acceptors required by metabolic processes depends not only on microbial growth rate but also on the coefficient of proportionality between substrates and electron acceptors which is given by the stoichiometric coefficient of the redox reaction. Changes in concentrations of electron acceptors are caused by both microbial growth and consumption by endogenous respiration. The rate of consumption of the *q*th electron acceptor due to microbial processes, B_q, is given by:

$$B_q = \frac{\partial C_a^q}{\partial t} = -\sum_{i=1}^{N_b}\sum_{j=1}^{N_b^i} \frac{f_a^{i,j,q}}{Y_s^{i,j,p}} \frac{\partial C_b^i}{\partial t}\Big|_{growth} + \sum_{i=1}^{N_b} f_{ea}^i \frac{\partial C_b^i}{\partial t}\Big|_{endogenous} \quad (16)$$

where $f_a^{i,j,q}$ is the coefficient of proportionality defined as the ratio of the rate of consumption of electron acceptor to that of the substrate, and f_{ea}^i is the electron acceptor consumption coefficient for the endogenous respiration of the *i*th microbial species.

Some microorganisms such as *Nitrosomonas* and *Nitrobacter* in the nitrogen cycle require inorganic nutrients and rely not only on organic or inorganic carbon but also on inorganic nutrients in order to yield energy. Changes in concentrations of nutrients are caused also by microbial growth. The rate of consumption of the *r*th nutrient, B_r, is given by:

$$B_r = \frac{\partial C_n^r}{\partial t} = -\sum_{i=1}^{N_b}\sum_{j=1}^{N_b^i} \frac{f_n^{i,j,r}}{Y_s^{i,j,p}} \frac{\partial C_b^i}{\partial t}\Big|_{growth} \quad (17)$$

where $f_n^{i,j,r}$ is the coefficient of proportionality between consumed substrate and consumed nutrient.

To illustrate the previous concepts, let us consider Iron Reducing Bacteria (IRB) which grow by oxidizing dissolved organic carbon (DOC) and reducing ferric minerals. Let R_B be the microbial growth rate. The rate of substrate consumption, R_{DOC}, is given by

$$R_{DOC} = -\frac{R_B}{Y_B} \quad (18)$$

where Y_B is the yield coefficient of DOC to IRB. Oxidation of DOC usually yields bicarbonate production. Then, the rate of bicarbonate, $R_{HCO_3^-}$, is calculated as $R_{HCO_3^-} = -Y_{HCO_3^-} R_{DOC}$ where $Y_{HCO_3^-}$ is the yield coefficient of HCO_3^- from DOC. The consumption rate of Fe^{3+}, $R_{Fe^{3+}}$, is given by $R_{Fe^{3+}} = f_a R_{DOC}$ where f_a is the proportionality coefficient of Fe^{3+} and DOC in the redox process. In general, the proportionality coefficient is equal to the stoichiometric coefficient. When complex macromolecular organic matter is used as substrate, however, the stoichiometric coefficient may be unknown.

4. Numerical Solution Techniques

The numerical formulation for solving the coupled equations of solute transport, chemical reactions and microbial processes is based on the Sequential Iteration Approach (SIA) (Yeh and Tripathi, 1991; Simunek and Suarez, 1994; Walter *et al.*, 1994a,b; Lichtner, 1996; Xu *et al.*, 1999) in which transport and chemical equations are solved separately in a sequential manner. Transport equations are solved first, followed by those of chemical and microbial reactions. This sequential process is repeated until convergence is attained for a prescribed tolerance. The key point of SIA is therefore the sequential solution of three independent sets of equations: (a) transport equations which are solved in a component manner, (b) chemical equations, and c) microbial reactions. The latter two are solved nodewise. These three sets of equations are coupled by means of reaction sink /source terms which are updated during the iterative process. Yeh and Tripathi (1989) discuss the explicit and implicit schemes for SIA. The implicit scheme is more advantageous than the explicit because it is less prone to get negative concentrations, can be applied to steady-state problems and has a faster convergence rate. The implicit scheme, however, requires a transport operator slightly different than the

standard transport operator. Our formulation uses a mixed explicit-implicit scheme which is based on the standard transport operator and has adequate convergence properties (Xu, 1996). This scheme derives from rewriting Eq. 2 as

$$\nabla\cdot\left(\theta\mathbf{D}\nabla C_j^{s+1/2}\right)-\mathbf{q}\cdot\nabla C_j^{s+1/2}+w\left(C_j^{*}-C_j^{s+1/2}\right)+\theta R_j^{s}= =\theta\frac{\partial C_j^{s+1/2}}{\partial t}\qquad j=1,\ldots,N_C \tag{19}$$

where superscript s denotes the transport plus reaction iteration number. A transport plus reaction iteration consists of two stages, a transport stage denoted by s+½ (it should be noticed that ½ does not mean Δt/2 where Δt is the time step) and a reaction stage denoted by s+1.

Since chemical and biological reaction sink/source terms, R_j^s, do not depend on $\mathbf{C}_j^{s+1/2}$, Eq. 2 are linear and have the same structure as standard transport equations of conservative solutes. These equations are solved with Galerkin finite elements (*Xu*, 1996) and using a finite difference scheme for time derivatives. The system of equations for the j-th component is given by:

$$\left[\eta\mathbf{E}+\frac{\mathbf{F}}{\Delta t}+\mathbf{H}\right]\mathbf{C}_j^{k+1,s+1/2}= =\mathbf{g}_j^{k+1}+\mathbf{R}_j^{k+1,s}+\left[(\eta-1)\mathbf{E}+\frac{\mathbf{F}}{\Delta t}+\mathbf{H}\right]\mathbf{C}_j^{k} \tag{20}$$

where η is a time weighting parameter (η=0 for explicit, η =1 for implicit), **E** is a (N_d x N_d) matrix containing dispersion and advection terms where N_d is the number of nodes of the finite element grid, **F** is also a (N_d x N_d) matrix of storage terms, $\mathbf{C}_j^{k+1,s+1/2}$ is a column vector of nodal concentrations at the (s+1/2) stage of the *(k+1)*th time step, $\mathbf{R}_j^{k+1,s}$ is the column vector of reaction sink/source terms which are derived from the solution of the chemical system at the *s*th iteration, $\mathbf{g}_j^{k+1}$ is a column vector containing boundary terms as well as external fluid sink/source terms, $\Delta t = t^{k+1} - t^k$, and superscript k denotes time step. The actual expressions of **E**, **F** and $\mathbf{g}_j^{k+1}$ are given by Xu (1996). **H** is a matrix containing first-order derivative terms of kinetic reaction rates with respect to concentrations for SIA-1 (Zhang, 2001). It is equal to zero for standard SIA.

Eq. (20) is solved separately for each one of the microbial species and chemical components. Computed component concentrations, $\mathbf{C}_j^{k+1,s+1/2}$, are then used to update total analytical concentrations, $\mathbf{T}_j^{k+1,s+1/2}$, which include contributions of precipitated, exchanged and sorbed species in addition to total dissolved concentrations. By solving chemical equations one obtains new values of dissolved concentrations, $\mathbf{C}_j^{k+1,s+1}$, and reaction terms, $\mathbf{R}_j^{k+1,s+1}$, which are compared to $\mathbf{C}_j^{k+1,s}$ and $\mathbf{R}_j^{k+1,s}$, respectively to check for convergence. Sequential solution of transport and chemical equations is repeated until prescribed convergence criteria are satisfied both in terms of dissolved concentrations and reactive terms.

Both geochemical and microbial processes are governed by nonlinear equations which are usually solved with the Newton-Raphson Iterative Method (NRIM). The use of the NRIM for solving chemical equations is described in Samper *et al.* (2003a). The NRIM used for solving the microbial ecosystem in BIO-CORE$^{2D©}$ is described by Zhang (2001) and is summarized here. In a time period, Δt, microbial growth induces a biomass change given by:

$$\Delta C_b^i=\int_t^{t+\Delta t}\frac{\partial C_b^i}{\partial t}dt \tag{21}$$

where $\frac{\partial C_b^i}{\partial t}$ is given by Eq.(14). If Δt is small enough, $\frac{\partial C_b^i}{\partial t}$ can be considered constant over Δt. Therefore, one has:

$$\Delta C_b^i=\frac{\partial C_b^i}{\partial t}\Delta t\qquad i=1,\ldots,N_b \tag{22}$$

Changes in substrate, electron acceptor and nutrient concentrations can be computed in a similar manner from their rates B_p, B_q and B_γ given in Eq. (15) to (17):

$$\Delta C_s^p=B_p\Delta t\quad(p=1,\ldots,N_s) \tag{23}$$

$$\Delta C_a^q=B_q\Delta t\quad(q=1,\ldots,N_a) \tag{24}$$

$$\Delta C_n^r=B_r\Delta t\quad(r=1,\ldots,N_n) \tag{25}$$

where C_b^i, C_s^p, C_a^q and C_n^γ are concentrations of biomass, substrates, electron acceptors and nutrients, respectively. Concentrations of biomass, substrates, electron acceptors and nutrients at time $t+\Delta t$ are computed from:

$$\begin{cases}C_b^i={}^0C_b^i+\Delta C_b^i={}^0C_b^i+\dfrac{\partial C_b^i}{\partial t}\Delta t\\ C_s^p={}^0C_s^p+\Delta C_s^p={}^0C_s^p+B_p\Delta t\\ C_a^q={}^0C_a^q+\Delta C_a^q={}^0C_a^q+B_q\Delta t\\ C_n^r={}^0C_n^r+\Delta C_n^r={}^0C_n^r+B_r\Delta t\end{cases} \tag{26}$$

where superscript "0" denotes concentrations at time *t*. These equations can be written in residual form as:

$$\begin{cases}F_b^i=C_b^i-{}^0C_b^i-\dfrac{\partial C_b^i}{\partial t}\Delta t=0\\ F_s^p=C_s^p-{}^0C_s^p-B_p\Delta t=0\\ F_a^q=C_a^q-{}^0C_a^q-B_q\Delta t=0\\ F_n^r=C_n^r-{}^0C_n^r-B_r\Delta t=0\end{cases} \tag{27}$$

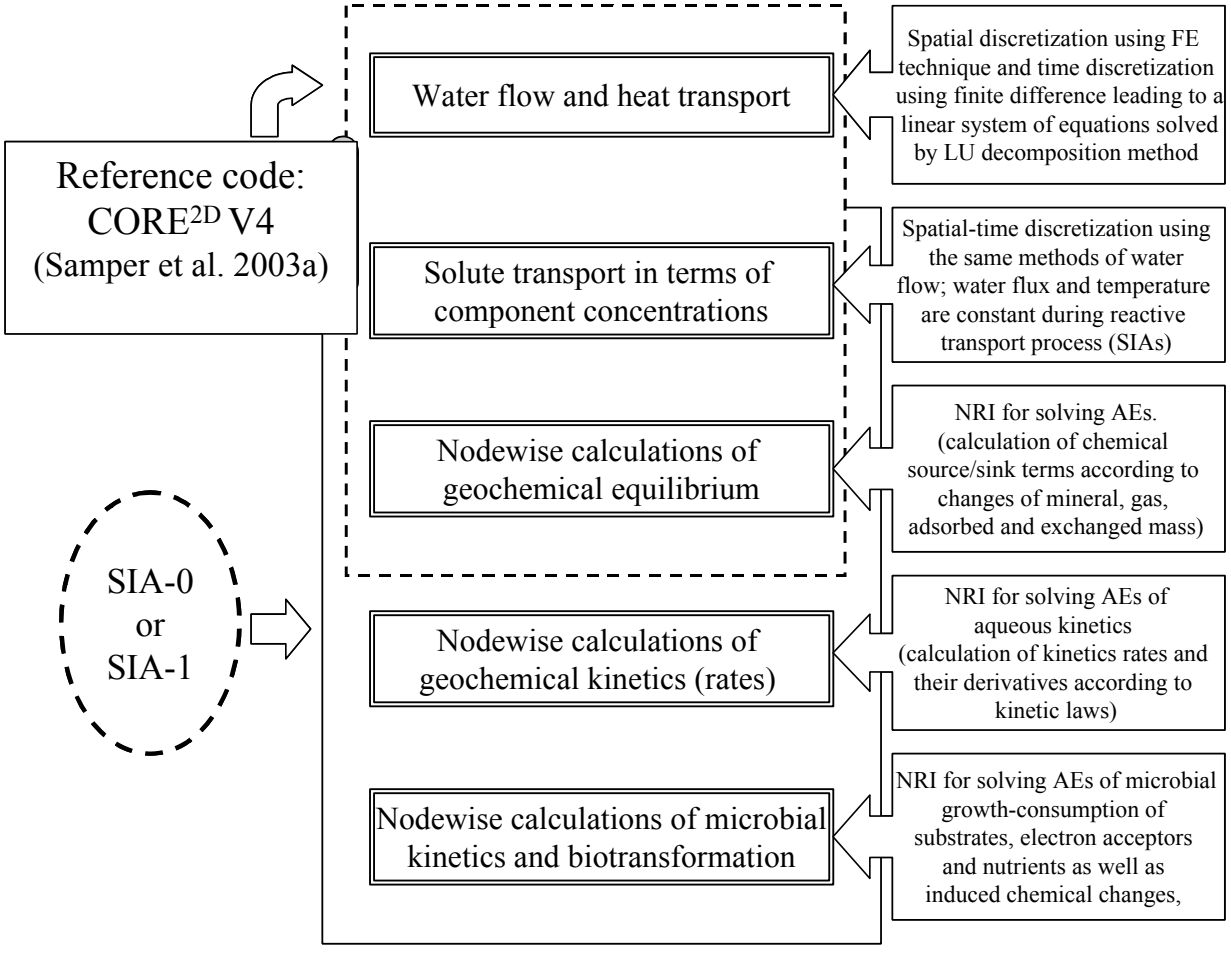

Fig. 1.- Main structure of BIO-CORE$^{2D©}$ (FE = finite element, NRI = Newton-Raphson Iteration, SIAs = SIA-0 + SIA-1 = Sequential Iteration Approaches and AEs = Algebraic Equations) (from Zhang, 2001).
Fig. 1.- Estructura principal de BIO-CORE$^{2D©}$ (FE = elementos finitos, NRI = Iteración Newton-Raphson, SIAs = SIA-0 + SIA-1 = Aproximación de iteración secuencial y AEs = Ecuaciones algebraicas) (Zhang, 2001).

This set of $N_b+N_s+N_a+N_n$ equations are solved using the NRIM. Details on the Jacobian matrix can be found in Zhang (2001). The solution of Equations (27) provides concentrations at $(t + \Delta t)$.

BIO-CORE$^{2D©}$ is structured in five major modules: (1) Water flow and heat transfer, (2) Solute transport, (3) Geochemical equilibrium calculations, (4) Geochemical kinetic calculations and (5) Microbial kinetics. They are solved sequentially as illustrated in figure 1.

5. Modeling a synthetic experiment for benchmarking BIO-CORE$^{2D©}$

A synthetic experiment is used here to illustrate the capabilities of coupled microbial and reactive transport models. It corresponds to a 1-D column with equilibrium aqueous complexation, kinetic biodegradation and kinetic sorption/desorption reactions. It was originally developed according to a real batch biodegradation experiment reported by Tebes-Stevens *et al.* (1998) and later has been used by others as a benchmark case to verify PHREEQC (Parkhurst and Appelo, 1999), HBGC123D (Savage and Yeh, 1998), MULTIFLO (Lichtner, 1998), RAFT (Chilakapati, 1998) and BIO-CORE$^{2D©}$ (Zhang, 2001). The column is 10 m long and contains a porous material having a porosity of 0.4, a dispersivity of 0.05 m and a bulk density of 1.5 Kg/L. Porewater velocity is 1 m/hr.

A Neuman boundary condition is used at the inlet of the column, while the end of the column is a free outflow boundary. The duration of the simulation is 75 hours. For the first 20 hours of the simulation, a pulse containing cobalt (Co^{2+}) and nitrilotriacetate (NTA^{3-}) is injected at the column inlet. After 20 hours, the background (initial) solution water is introduced at the inlet until the experiment ends after 75 hours.

The chemical system contains six aqueous components and three immobile components. Initial and boundary component concentrations are listed in Table 1. Stoichio-

Component	Type	Pulse concentration	Background concentration
H^+	Aqueous	pH = 6	pH = 6
$H_2CO_{3(aq)}$	Aqueous	4.9×10^{-7} mol/L	4.9×10^{-7} mol/L
NH_4^+	Aqueous	0.0	0.0
O_2	Aqueous	3.125×10^{-5} mol/L	3.125×10^{-5} mol/L
NTA_3^-	Aqueous	5.23×10^{-6} mol/L	0.0
Co^{2+}	Aqueous	5.23×10^{-6} mol/L	0.0
Biomass	Immobile	—	1.36×10^{-4} g/L
CoNTA(ads)	Immobile	—	0.0
Co(ads)	Immobile	—	0.0

Table 1. Initial and boundary concentrations of components.
Tabla 1. Concentraciones iniciales y de contorno de los componentes.

Complex	Stoichiometric coefficients						
	H^+	H_2CO_3	NH_4^+	O_2	NTA_3^-	Co^{2+}	log Keq
H_3NTA	3	0	0	0	1	0	-14.9
H_2NTA^-	2	0	0	0	1	0	-13.3
$HNTA^{2-}$	1	0	0	0	1	0	-10.3
$CoNTA^-$	0	0	0	0	1	1	-11.7
$CoNTA_2^{4-}$	0	0	0	0	2	1	-14.5
$CoOHNTA^{2-}$	-1	0	0	0	1	1	-0.5
$CoOH^+$	-1	0	0	0	0	1	9.7
$Co(OH)_2^-$	-2	0	0	0	0	1	22.9
$Co(OH)_3^-$	-3	0	0	0	0	1	31.5
HCO_3^-	-1	1	0	0	0	0	6.35
$CO3^{2-}$	-2	1	0	0	0	0	16.68
$NH_3(aq)$	-1	0	1	0	0	0	9.3
OH^-	-1	0	0	0	0	0	14.0

Table 2. Stoichiometric coefficients and equilibrium constants for aqueous complexes.
Tabla 2. Coeficientes estequiométricos y constantes de equilibrio para los complejos acuosos.

metric coefficients and equilibrium constants for the 13 secondary species are listed in Table 2.

Biodegradation of the complex $HNTA^{2-}$ is given by the following reaction:

$$HNTA^{2-} + 1.620\ O_2 + 1.272\ H_2O + 2.424\ H^+ \Longrightarrow 0.576\ C_5H_7O_2N + 3.120\ H_2CO_3 + 0.424\ NH_4^+$$

The rate of substrate degradation ($R_{HNTA^{2-}}$) is modeled by dual Monod kinetics:

$$R_{HNTA^{2-}} = -\mu_m X_m \frac{[HNTA^{2-}]}{K_s + [HNTA^{2-}]} \frac{[O_2]}{K_A + [O_2]} \qquad (28)$$

where X_m is biomass concentration, ($HNTA^{2-}$) is the concentration of $HNTA^{2-}$ and [O_2] is the concentration of oxygen. Biodegradation parameters are listed in Table 3. The net rate of microbial growth (R_{cells}) is given by the synthesis rate (which is equal to the rate of degradation of the substrate multiplied by a yield coefficient) minus a first-order decay rate:

$$R_{cells} = -YR_{HNTA2-} - bXm \qquad (29)$$

where *Y* and *b* are yield and decay coefficients, respectively.

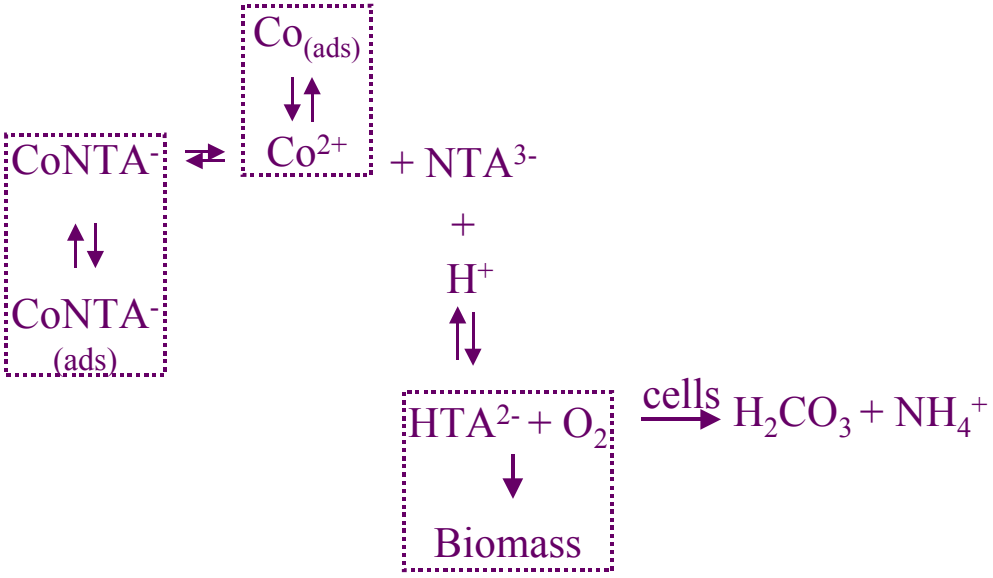

Fig. 2.- Schematic illustration of the main reactions in the NTA synthetic case.
Fig. 2. Ilustración esquemática de las principales reacciones en el caso sintético NTA.

Sorption reactions obey a linear kinetic model given by the following rate expression:

$$R_{X_{aq}} = \frac{d[X]}{dt} = -k_m([X] - \frac{\overline{X}}{K_d}) \quad (30)$$

where [X] denotes aqueous concentration of species X in mol/L, $\overline{X}$ is adsorbed concentration in mol/g, k_m is the mass transfer coefficient in hr^{-1}, and K_d is the distribution coefficient for linear equilibrium adsorption. The corresponding rate for adsorbed species is given by:

$$R_{X_{ad}} = \frac{d\overline{X}}{dt} = -\frac{\theta}{\rho}\frac{d[X]}{dt} = \frac{\theta}{\rho}K_m([X] - \frac{\overline{X}}{K_d}) \quad (31)$$

Free dissolved cobalt (Co^{2+}) and $CoNTA^-$ are retarded due to sorption. The mass transfer coefficient is equal to 1 hr^{-1} for both sorption reactions. Distribution coefficients for Co^{2+} and $CoNTA^-$ are be equal to 5.07×10^{-3} L/g and 5.33×10^{-4} L/g, respectively. These distribution coefficients amount to retardation coefficients, R_f, of 20 for Co^{2+} and 3 for $CoNTA^-$, respectively. The main reactions of the system are illustrated in figure 2. This problem is solved with BIO-CORE$^{2D©}$ with a regular grid of $\Delta x = 0.1$ m and using an automatic time stepping algorithm.

Biodegradation causes an increase in pH to a maximum value of about 6.7 at the end of the column after 30 hours. This increase in pH results in a redistribution of species. As pH rises, $CoNTA^-$ forms at the expense of Co^{2+} and $HNTA^{2-}$. The rise in pH affects the results of the simulation in two ways. Since $HNTA^{2-}$is the biodegradable form of NTA, the increase in pH causes a decrease in the overall amount of biodegradation in the column. This is confirmed by the concentration breakthrough curves of biomass at any given point along the column. On the other hand, since $CoNTA^-$ ($R_f \approx 3$) does not adsorb as strongly as the uncomplexed cobalt (Co^{2+}, $R_f \approx 20$), the increase in the concentration of $CoNTA^-$ relative to that of Co^{2+} allows cobalt to migrate through the column more quickly. The results of BIO-CORE$^{2D©}$ coincide with those obtained by Tebes-Stevens *et al.* (1998) with FEREACT (Fig. 3 and 4).

Parameter	Description	Value
K_S	half-saturation constant for substrate	7.64×10^{-7} mol/L
K_A	half-saturation constant for electron donor	6.25×10^{-6} mol/L
μ_m	specific rate of substrate utilization	1.407×10^{-3}mol NTA/g cells/hr
Y	microbial yield coefficient	65.14 g cells/mol of NTA
b	microbial decay coefficient	0.00208 hr^{-1}

Table 3. Biodegradation rate parameters.
Tabla 3. Parámetros de tasa de biodegradación.

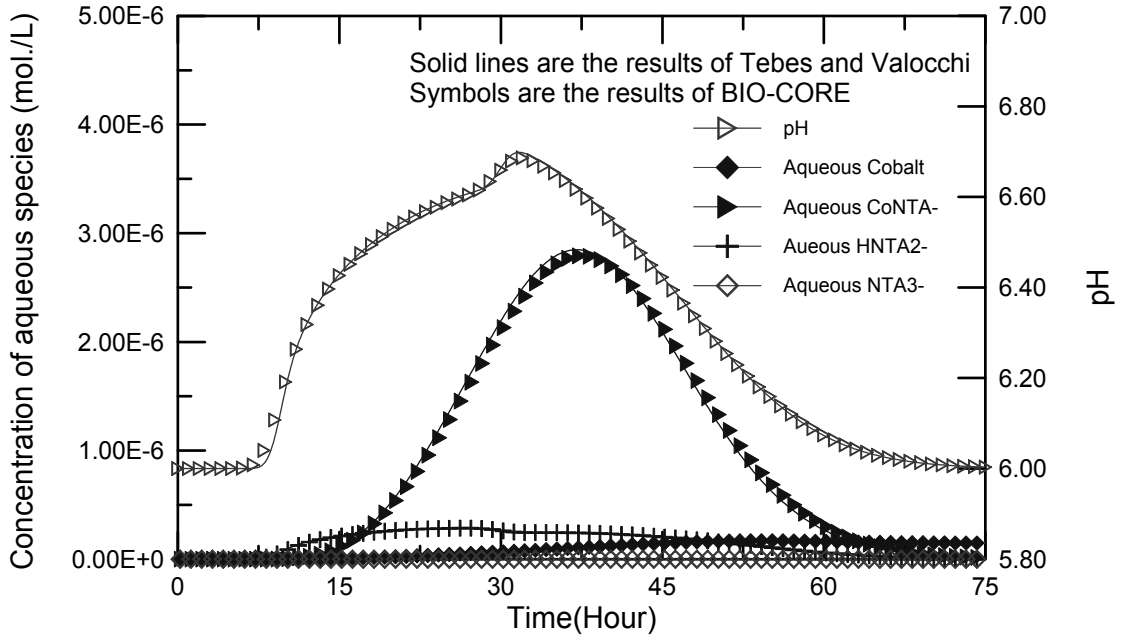

Fig. 3.- Concentration breakthrough curves of aqueous species at the end of the column.
Fig. 3.- Curvas de llegada de la concentración de las especies acuosas al final de la columna.

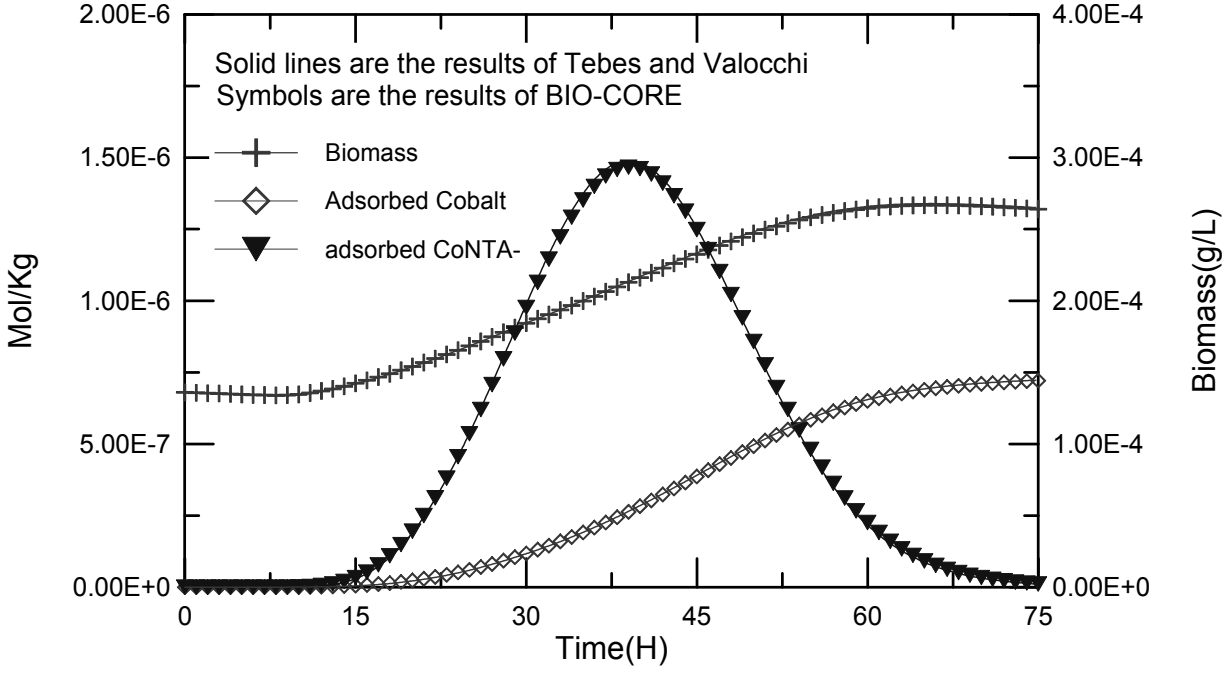

Fig. 4.- Concentration breakthrough curves of adsorbed species at the end of the column.
Fig. 4.- Curvas de llegada de la concentración de las especies adsorbidas al final de la columna.

6. Modeling iron and sulfate reduction in Boom clay

The CERBERUS experiment was carried out at the HADES (High Activity Disposal Experimental Site) facility excavated in Boom clay formation at Mol (Belgium) to evaluate the effect of heating and radiation in Boom clay. The test was performed in a cased well drilled at 223 m depth and lasted from 1989 to 1994. A ^{60}Co source of 400 TBq and two heaters were emplaced inside the well (Fig. 5).

The clay was excavated, and a 760 mm diameter casing was installed to a depth of 2 m. Then, a 450 mm diameter

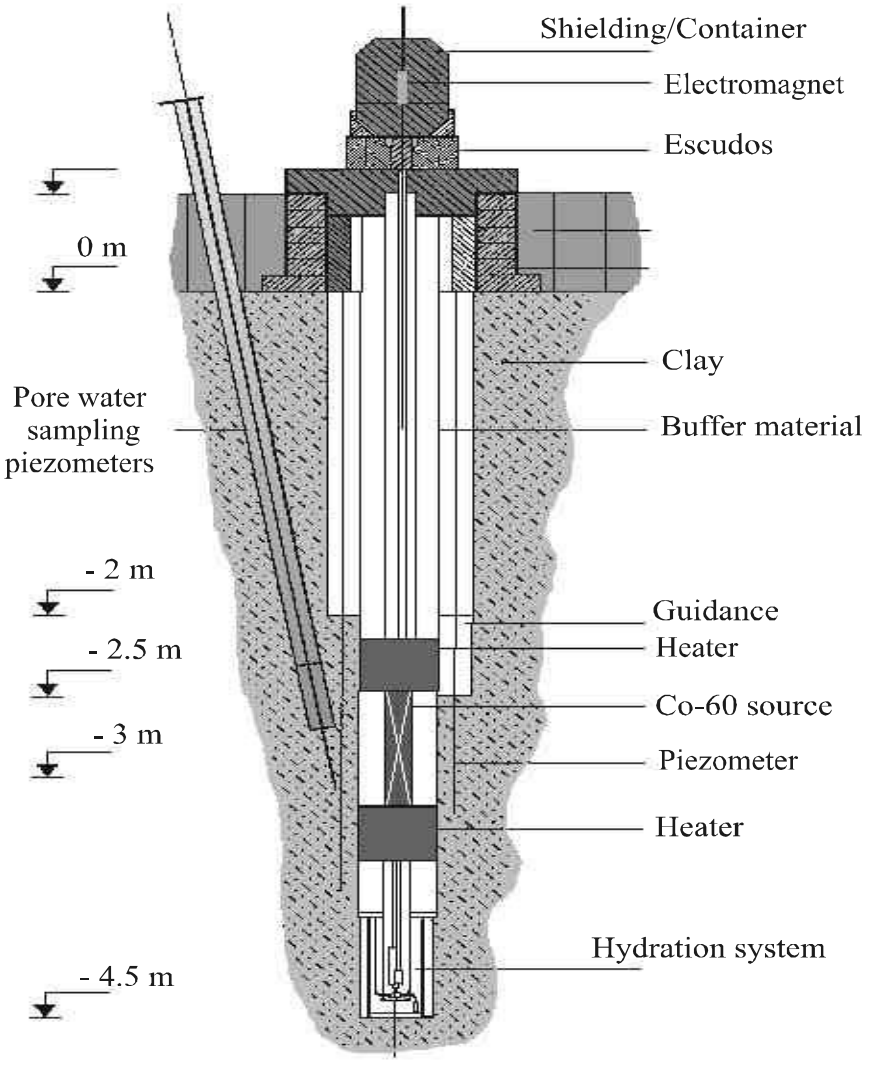

Fig. 5.- Scheme of CERBERUS experiment (modified from Noynaert *et al.*, 2000).
Fig. 5.- Esquema del experimento CERBERUS (modificado de Noynaert *et al.*, 2000).

casing was installed to a depth of 4.5 m below the extrados of the HADES gallery. *In situ* measurements of dose rates, temperatures, pore–water pressures and pH/Eh values were performed. Pore–waters were sampled during six campaigns in two piezometers located at 0.1 m from the wall and 0.303 m from the central axis of the test well, approximately 3 m below the gallery extrados.

Boom clay in Mol, Belgium, is composed of the following primary minerals (by weight percent): illite, 32.7%; montmorillonite, 12.5%; kaolinite, 10.1%; quartz, 20%; and K-feldspar, 6%, with carbonates and pyrite as secondary minerals. Pyrite was found to precipitate in the near field of Boom clay during the experiment (see Fig. 6). This precipitation was associated with the bound organic matter (3.0-4.6% content) in the Boom clay matrix.

Noynaert *et al.* (2000) presented a coupled thermo-hydro-geochemical (THC) model of the CERBERUS experiment which accounts for heating, radiation, solute diffusion and a suite of geochemical reactions including: aqueous complexation, acid-base, redox, mineral dissolution/precipitation, cation exchange and gas dissolution/ex-solution. The model reproduces the trends of some chemical species, but fails to fit sulfate, bicarbonate and iron species.

During the excavation of the experimental well, the Boom clay was aerated, inducing aerobic biodegradation of the bound organic matter with release of sulfide and CO_2. In aerobic conditions, sulfide was immediately oxidized to sulfate. Consequently, the sulfate concentration near the experiment well was substantially higher (9.13×10^{-3} mol/L) than that of the undisturbed background value (3×10^{-5}–1.448×10^{-4} mol/L). After the well was cased, the clay was isolated from the air. Aerobic biodegradation was inhibited and iron and sulfate reduction occurred. These processes yielded also an increase in bicarbonate concentration. Sulfate concentration decreased with radial distance from the well. Diffusive sulfate dissipation also reduced the near–field sulfate concentration. Con-

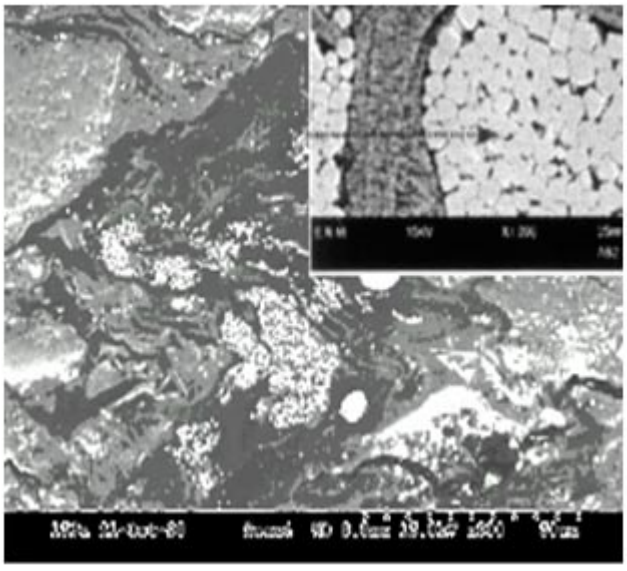

Fig. 6.- Organic matter (dark parts) in clay matrix associated with crystallization of pyrite (bright dots). Inset picture shows pyrite crystals in fossilized cells (modified from Noynaert *et al.*, 2000).

Fig. 6.- Materia orgánica (partes oscuras) en matriz arcillosa, asociada con cristalización de pirita (puntos brillantes). La figura más pequeña muestra cristales de pirita en fósiles (modificado de Noynaert *et al.*, 2000).

comitantly, iron reduction took place in areas with low sulfate concentrations. During the continuous reduction of sulfate and ferric iron, pyrite precipitated where reduced sulfur, HS-, encounters reduced iron, Fe(II).

Discrepancies of the THC model of Noynaert *et al.* (2000) are overcome when microbially-mediated iron and sulfate reduction are taken into account in a coupled thermo-hydro-bio-geochemical (THBC) model. The results of the THBC model for sulfate, bicarbonate and iron species greatly improve those of the THC model. Figure 7 illustrates the comparison of THC and THBC models for sulfate. In addition, contrary to the THC model which predicts pyrite dissolution, the results of the THBC model indicate that pyrite precipitates at the observation point (see Fig. 8). Such precipitation is consistent with experimental observations shown in Figure 6.

Model results confirm that microbial iron and sulfate reductions are key processes controlling the geochemical evolution of the near–field Boom clay, which is maintained in strongly reducing conditions (–330 to –250 mV). The radiation-induced oxygen is rapidly buffered and does not impact the near–field environment. Microbial iron and sulfate reduction are key processes to mitigate the impact of oxygen. Additional details of this case study are provided by Samper *et al.* (2006b).

7. Conclusions

Mathematical and numerical formulation of coupled water flow, heat and solute transport, and geochemical and biological processes in porous media has been presented. Such formulation has been implemented in biogeochemical reactive transport code, BIO-CORE$^{2D©}$, by adding microbiological processes into a nonisothermal reactive transport code CORE$^{2D©}$ (Samper *et al.*, 2003a). Capabilities of coupled hydrobiogeochemical models have been illustrated by means of a synthetic example dealing with equilibrium aqueous complexation, biodegradation and kinetic sorption/desorption reactions in a column experiment. BIO-CORE$^{2D©}$ numerical solutions reproduce those of FEREACT. It has been shown also how a coupled microbial reactive transport model of the CERBERUS experiment performed with BIO-CORE$^{2D©}$ overcomes the limitations of a purely reactive transport model by providing a plausible response to the observed decrease of dissolved sulfate concentrations and pyrite precipitation.

Acknowledgments

This work was supported by research projects funded by ENRESA and the RADWAS Program of the European Union (FEBEX I Project, FI4W-CT95-00008; FEBEX II Project, FIKW-CT-2000-0016; CERBERUS Project, FI4W-CT95-00006) through collaborative agreements with University of La Coruña (FEBEX Project, codes 703231 and 770045; Validation Project, code 703334). Funding for the development of reactive transport codes was also provided by the Spanish Science and Technology Commission (CICYT Project, HID98-0282). The second author thanks the University of La Coruña for providing a research scholarship during year 2000. We thank the two reviewers, Tianfu Xu and Albert Valocchi, for their constructive comments and suggestions which have improved the paper.

References

Appelo, C.A.J., Postma, D. (1993): *Geochemistry, Groundwater and Pollution*. Ed. Balkema, Rotterdam.

Ayora, C., Samper, J., Xu, T. (1995): *Reactive solute transport modeling: problem statement and hydrochemical model*, VI Simposio de Hidrogeología y Recursos Hidráulicos, Vol XIX, pp. 769-784.

Battistelli, A. (2004): Modeling Biodegradation of Organic Contaminants under Multiphase Condition with TMVOC-Bio. *Vadose Zone Journal,* 3:875-883.

Bear J. (1979): *Hydraulics of Groundwater*. McGraw-Hill, 569 pp.

Fig. 7.- Measured and computed time evolution of dissolved sulfate at the observation point considering only heating (H), heating and radiation (H&R) and heating+radiation +microbial processes.

Fig. 7.- Evolución temporal de las concentraciones de sulfato disuelto calculadas y medidas en el punto de observación para los modelos de: sólo calentamiento (H), calentamiento y radiación (H&R) y calentamiento, radiación y procesos microbianos.

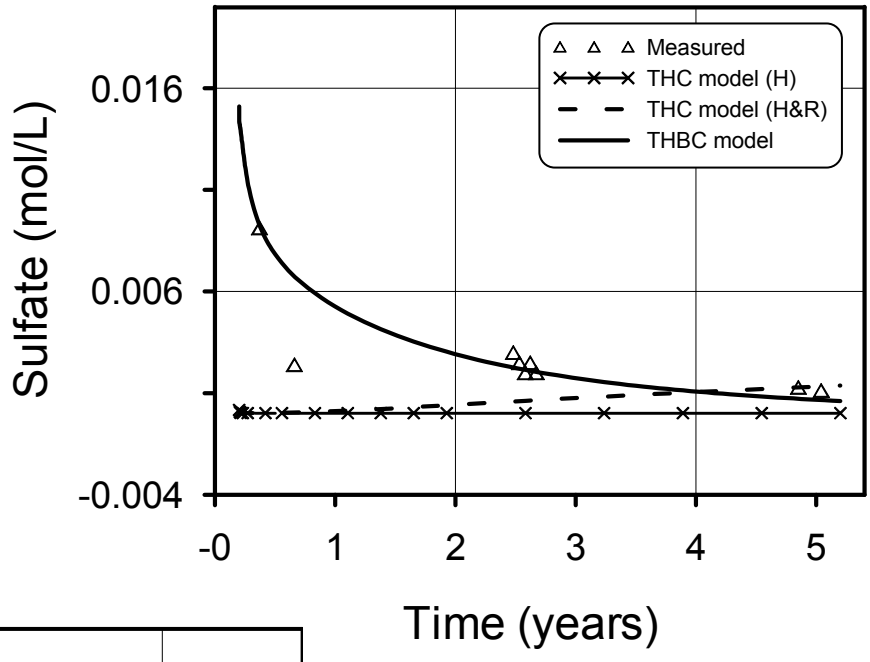

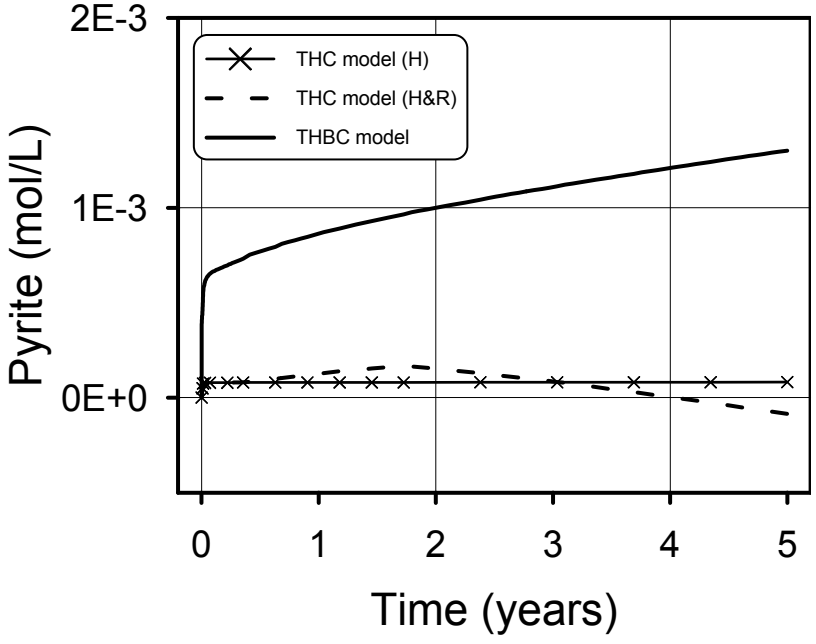

Fig. 8.- Time evolution of computed cumulative pyrite dissolution/precipitation at the observation point (negative values for dissolution and positive for precipitation) considering only heating (H), heating and radiation (H&R) and microbial processes.

Fig. 8.- Evolución temporal de los valores acumulados de disolución/precipitación de pirita en el punto de observación (valores negativos para disolución y positivos para precipitación) para los modelos de: sólo calentamiento (H), calentamiento y radiación (H&R) y calentamiento, radiación y procesos microbianos.

Brun, A. (1997): *Reactive transport modeling of coupled inorganic and organic processes in groundwater*. Ph. D. Dissertation. Department of Hydrodynamics and Water Resources, Technical University of Denmark, 184 pp.

Carnahan, C.L. (1990): Coupling of precipitation/dissolution reactions and mass diffusion via porosity changes. In: D.C, Melchior, R.L., Bassett (eds.): *Chemical Modeling of Aqueous Systems II*. American Chemical Society, Washington, D.C., pp. 234-242.

Cederberg, G.A., Street, R., Leckie, J.O. (1985): A groundwater mass transport and equilibrium chemistry model for multicomponent systems, *Water Resources Research*, 21(8): 1095-1104.

Chilakapati, A.B., Yabusaki, S., Szecsody, J., MacEvoy, W. (2000): Groundwater flow, multicomponent transport and biogeochemistry: development and application of a coupled process model. *Journal of Contaminant Hydrology*, 43: 303-325.

Dzombak, D.A., Morel, F.M.M. (1990): *Surface Complexation Modelling*. Wiley Interscience, New York.

Engesgaard, P. (2000): *Model for biological clogging in 3D, Brief user's manual and guide.* Department of Hydrodynamics and Water Resources, Danish Technology University.

Essaid, H., Bekins, A. (1997): *BIOMOC, A Multispecies Solute-Transport Model with Biodegradation*. U.S. Geological Survey. Water-Resources Investigations Report 97-4022, 68 pp.

Hunter, K.S., Wang, Y., van Cappellen, P. (1998): Kinetic Modeling of Microbially-Driven Chemistry of Subsurface Environments: Coupling Transport, Microbial Metabolism and Geochemistry. *Journal of Hydrology*, 209: 53-80.

Jennings, A.A., Kirkner, D.J., Theis, T.L. (1982): Multicomponent equilibrium chemistry in groundwater quality models. *Water Resources Research*, 18(4): 1089-1096.

Kirkner, D.C., Reeves, M. (1988): Multicomponent mass transport with homogeneous and heterogeneous chemical reactions: Effect of the chemistry on the choice of numerical algorithm, 1, Theory. *Water Resources Research*, 24 (1): 1719-1729.

Lasaga, A.C., Soler, J.M., Ganor, J., Burch, T.E., Nagy, K.L. (1994): Chemical weathering rate laws and global geochemical cycles. *Geochimica et Cosmochimica Acta*, 58: 2361-2386.

Lewandowski, Z., Stoodley, P., Altobelli, S., Fukushima, E. (1994): Hydrodynamics and Kinetics in Biofilm Systems - Recent Advances and New Problems. *Water Science and Technology*, 29: 223-229.

Lichtner, P.C., Seth, M. (1996): Multiphase-Multicomponent Nonisothermal Reactive Transport in Partially Saturated Porous Media. *Proceedings of the International Conference on Deep Geological Disposal of Radioactive Waste*, Canadian Nuclear Society, 3-133 to 3-142. Toronto, Ontario, Canada: Canadian Nuclear Society. TIC: 237969.

Lichtner, P.C., Steefel, S.I., Oelkers, E.H. (1996): Reactive Transport in Porous Media. *Reviews in Mineralogy*, 34: 83-100.

Mangold, D., Tsang, C. (1991): A Summary of Subsurface Hydrological and Hydrochemical models. *Reviews of Geophysics*, 29: 51-79.

Miller, C.W., Benson, L.V. (1983): Simulation of solute transport in a chemically reactive heterogeneous system: Model development and application. *Water Resources Research*, 19: 381-391.

Molinero, J., Samper, J., Zhang, G., Yang, C. (2004): Biogeochemical reactive transport model of the redox zone experiment of the Äspö hard rock laboratory in Sweden. *Nuclear Technology*, 148: 151–165.

Molz, F.J., Widdowson, M.A., Benefield, L.D. (1986): Simulation of Microbial growth Dynamics Coupled to Nutrient and Oxygen transport in Porous Media. *Water Resources Research*, 22(8): 1207-1216.

Monod, J. (1949): The growth of bacterial cultures. *Annual Review of Microbiology*, 3: 371-394.

Noynaert, L., de Cannière, P., De Bruyn, D., Volckaert, G., Put, M., Kursten, B., Sneyers, A., Van Iseghem, P., Beaucaire, C., Pitsch, H., Bouchet, A., Parneix, J.C., Samper, J., Delgado, J., Navarro, V., Montenegro, L., Zhang, G. (2000): *Heat and radiation effects on the near field of a HLW or spent fuel repository in a clay formation (CERBERUS Project)*. Final Report. EUR 19125 EN, 157 pp.

Parkhurst, D.L., Thorstenson, D.C., Plummer, L.N. (1980): *PHREEQE—A computer program for geochemcial calculations*. U.S. Geological Survey Water-Resource Investigations report 80-96, p.195 (Revised and reprinted August, 1990)

Parkhurst, D.L., Appelo, C.A.J. (1999): *User's guide to PHREEQC (Version 2) -- a computer program for speciation batch-reaction, one-dimensional transport, and inverse geochemical calculations*. U.S. Geological Survey Water-Resources Investigations Report 99-4259, 312 p.

Pruess, K., Battistelli, A. (2002): *TMVOC, a numerical simulator for three-phase non-isothermal flows of multicomponent hydrocarbon mixture in saturated-unsaturated heterogeneous media*. Report LBNL-49375. Lawrence Berkeley National Laboratory, Berkeley, California,USA.

Rathfelder, K.M., Lang, J.R., Abriola, LM. (2000): A numerical model (MISTER) for the simulation of coupled physical, chemical and biological processes in soil vapor extraction and bioventing systems. *Journal of Contaminant Hydrology*, 43: 239-270.

Reeves, H., Kirkner, D.J. (1988): Multicomponent mass transport with homogeneous and heterogeneous chemical reactions: Effects of the chemistry on the choice of numerical algorithm, 2, Numerical results. *Water Resources Research*, 24 (10): 1730-1739.

Rheinheimer, G. (1992): *Aquatic Microbiology*. 4th Edition, Published by John Wiley & Sons Ltd.

Rubin, J., James, R.V. (1973): Dispersion-affected transport of reacting solutes in saturated porous media: Galerkin method applied to equilibrium-controlled exchange in unidirectional steady water flow. *Water Resources Research*, 9: 1332-1356.

Rubin, J. (1983): Transport of reactive solutes in porous media: relation between mathematical nature of problem formulation and chemical nature of reactions. *Water Resources Research*, 19(5): 1231-1252.

Saaltink, M.W., Benet, I., Ayora, C. (1997): *RETRASO, Fortran code for solving 2D reactive transport of solutes, user's guide.* ETSI Caminos, Canales y Puertos, Univ. Politècnica de Catalanya and Inst. Ciencias de la Terra, CSIC, Barcelona.

Saaltink, M.W., Carrera, J., Ayora., C. (2001): On the behaviour of approaches to simulate reactive transport. *Journal of Contaminant Hydrology*, 48(3-4): 213-235.

Salvage, K.M., Yeh, G.T. (1998): Development and Application of a Numerical Model of Kinetic and Equilibrium Microbiological and Geochemical Reactions (BIOKEMOD). *Journal of Hydrology*, 209: 27-52.

Salvage, K.M., Yeh, G.T. (1999): *HydroBioGeoChemical 123D User's guide 1.1*. Department of Civil and Environmental Engineering. The Pennsylvania State University.

Samper, J., Yang, C., Montenegro, L. (2003a): *CORE^{2D} version 4: A code for non-isothermal water flow and reactive solute transport. Users Manual*. Universidad de La Coruña, Spain.

Samper, J, Molinero, J., Yang, C., Zhang, G. (2003b): *Redox Zone II: Coupled modeling of groundwater flow, solute transport, chemical reactions and microbial processes in the Äspö Island*. SBK Technical Report TR-03-16, 126 pp.

Samper, J., Yang, C., Molinero J., Bonilla, M. (2006a): Modelling microbially-mediated consumption of dissolved oxygen after backfilling a high level waste repository. *Journal of Contaminant Hydrology* (submitted).

Samper, J., Montenegro, L., Zhang, G. (2006b): Coupled thermo-hydro-bio-geochemical reactive transport model of the CERBERUS heating and radiation experiment in Boom clay. Applied Geochemistry (submitted).

Simunek, J., Suares, D.L. (1994): Two-dimensional transport model for variably saturated porous media with major ion chemistry. *Water Resources Research*, 30(4): 1115-1133.

Steefel, C.I., Lasaga, A. (1990): The evolution of dissolution patterns: Permeability change due to Coupled Flow and Reaction. In: Melchior, D., Bassett, R.L. (eds.): *Chemical Modelling of Aqueous Systems II*, American Chemical Society (Chapter 16): 212-225.

Steefel, C.I., Lasaga, A.C. (1994): A coupled model for transport of multiple chemical species and kinetic precipitation/dissolution reactions with applications to reactive flow in single phase hydrothermal system. *American Journal of Science*, 294: 529-592.

Tebes-Stevens, C., Valocchi, A.J., van Briesen, J.M., Rittmann, B.E. (1998): Multicomponent Transport with Coupled Geochemical and Microbiological Reactions: Model Description and Example Simulations, *Journal of Hydrology*, 209: 8-26.

Valocchi, A.J., Street, R.L., Roberts, P.V. (1981): Transport of ion-exchanging solutes in groundwater: Chromatographic theory and field simulation. *Water Resources Research*, 17(5): 1517-1527.

Walter, A.L., Frind, E.O., Blowes, D.W., Ptacek, C.J., Molson, J.W. (1994a): Modeling of multicomponent reactive transport in groundwater. 1. Model development and evaluation. *Water Resources Research*, 30(11): 3137-3148.

Walter, A.L., Frind, E.O., Blowes, D.W., Ptacek, C.J., Molson, J.W. (1994b): Modeling of multicomponent reactive transport in groundwater. 2. Metal mobility in aquifers impacted by acidic mine tailings discharge. *Water Resources Research*, 30(11): 3149-3158.

Xu, T. (1996): *Modeling Non-isothermal multi-component reactive solute transport through variably saturated porous media*. Ph. D. Dissertation. University of La Coruña, Spain.

Xu, T., Samper, J., Ayora, C., Manzano, M., Custodio, E. (1999): Modeling of Non-Isothermal Multi-Component Reactive Transport in Field Scale Porous Media Flow System. Journal *of Hydrology*, 214(1-4): 144-164.

Xu, T., Sonnenthal, E., Spycher, N., Pruess, K. (2006): TOUGHREACT — A simulation program for non-isothermal multiphase reactive geochemical transport in variably saturated geologic Media: applications for geothermal injectivity and CO_2 geologic sequestration. *Computers and Geosciences*, 32: 145-165.

Yang, C. (2006): *Conceptual and numerical coupled Thermal-Hydro-Bio-Geochemical Models for three-dimensional porous and fractured media*. Ph.D. Dissertation, University of La Coruña, Spain, 400pp.

Yeh, G.T., Tripathi, V.S. (1989): A critical evaluation of recent developments of hydrogeochemical transport models of reactive multichemical components. *Water Resources Research*, 25(1): 93-108.

Yeh, G.T., Tripathi, V.S. (1991): A model for simulating transport of reactive multispecies components: model development and demonstration, *Water Resources Research*, 27(12): 3075-3094.

Zhang, G. (2001): HydroBioGeochemical Models in Porous Media. Ph.D. Dissertation, University of La Coruña, Spain, 368 pp.

Zhang, G., Samper, J. (2001a): Biohydrogeochemistry: A New Face of Groundwater Chemistry. *Proceedings of the Symposium Las Caras Del Agua Subterranea*. Barcelona, September 2001.

Zhang, G., Samper, J. (2001b): *BIO-CORE$^{2D©}$: A Code For Water Flow and Reactive Transport Including Surface Microbial Processes-User's Manual*. Technical Report, University of La Coruña, Spain.